Glycoconjugate Journal 15, 697–712 (1998)

Structure-function relations of heparin-mimetic sulfated xylan oligosaccharides: inhibition of Human Immunodeficiency Virus-1 infectivity *in vitro*

Audrey Larack Stone[1]*, Derek J. Melton[1] and Marc S. Lewis[2]

[1] *Laboratory of Developmental and Molecular Immunity, National Institute of Child Health and Human Development, NIH and*
[2] *Biomedical Engineering and Instrumentation Program, NCRR, NIH, 9000 Rockville Pike, Bethesda, MD 20892*

Heparins/heparan sulfates modulate the function of proteins and cell membranes in numerous biological systems including normal and disease processes in humans. Heparin has been used for many years as an anticoagulant, and anticoagulant heparin-mimetics were developed several decades ago by chemical sulfation of non-mammalian polysaccharides, e.g., an antithrombotic sulfated xylan. This pharmaceutical, which comprises a mixture of sulfated oligoxylans, also mimics most other biological actions of natural heparins *in vitro*, including inhibition of the human immunodeficiency virus, but the molecular basis for these actions has been unclear. Here, numerous Components of the sulfated oligoxylan mixture were isolated and when bioassayed in the case of anti-HIV-1 infectivity revealed that a structural specificity underlines the capacity of sulfated xylan to inhibit HIV-1, rather than a non-specific mechanism. Components were isolated by chromatographic fractionation through Bio-Gel P10 in 0.5M ammonium bicarbonate. This fractionation revealed an elution range associated with apparent molecular weights of $\sim$22 000 to <1500 relative to standard heparin and heparan sulfates and newly prepared sulfated oligosaccharide standards. Components were characterized by metachromatic absorption spectroscopy, ultracentrifugation, GlcA analysis, and potency against HIV-1 infectivity, both in the tetrazolium cytotoxicity assay and in syncytium-forming assays, in CD4-lymphocytes. Structural specificity was indicated by the differential potencies exhibited by the Components: Highest activity (cytotoxicity) was exhibited by Components in the chromatographic region $\geqslant \sim$5500 in mass (50% effective (inhibitory) concentration = 0.5–0.7 μg ml^{-1} in the first fractionation series, and 0.1–0.5 μg ml^{-1} in a second series). The potency declined sharply below $\sim$5400 in mass, but with an exception; a second structure exhibiting relatively high potency eluted among low-mass oligosaccharides which had an average size of $\sim$ a nonomer. Components displayed differential potencies also against the syncytium-forming infectivity of HIV-1. The high potency against syncytium-formation was retained by Components down to a minimum size of about 4500 in mass, smaller than the $\geqslant \sim$5400 required above. One in ten of the β1,4-linked xyloses in the native xylan are substituted with a monomeric α1,2 DGlcA branch. We have speculated that pharmaceutical actions of sulfated xylan might be related to structures involving the α-D linked substituents and this was examined using a space-filling model of a sulfated octaxylan and by analyses of Components for GlcA content. Understanding structure/function relations in the heparin-like actions of these agents would be of general significance for the careful examination of their potential clinical usefulness in many human processes modulated by heparins, including AIDS.

***Keywords*: Heparin-mimetic oligosaccharides, anti-HIV-1 capacity of components of sulfated xylan, mass of sulfated oligosaccharides by equilibrium-ultracentrifugation.**

Introduction

The complex biosynthesis of the sulfated α-D glucosamine: uronic acid-disaccharide repeating structures of the heparin class of biopolymers, elucidated largely by Lindahl and coworkers, is well known [1–3, 4 (Review)]. However, an underlying structural design that would encompass the specific structures for heparins in their numerous protein and cell-membrane modulatory functions remains to be elucidated. The structure/function relation of one biological function of heparin (heparin as an activator of the blood serine protease inhibitor, antithrombin) has been elucidated explicitly at the molecular level starting with the work of

* To whom correspondence should be addressed. Tel: 301-496-8846; Fax: 301-480-9862; E-mail: ASTONE@helix.NIH.gov

Rosenberg and coworkers in the 1970s, [5–8, 9 (Review)]. Heparin, isolated from pig mucosa as a mixture of glycosaminoglycan chains heterogeneous in size and anionic density, had been an anticoagulant pharmaceutical in clinical use for many years. This work revealed that the anticoagulant function of the heparin obtains not from the structural properties of the bulk preparation of glycan chains, but instead resides specifically in a small portion of the molecules. Subsequent studies showed that these molecules contain a short specific binding sequence of ~ 3 disaccharides which provides most of the binding energy for the reaction between heparin and antithrombin and alone produces a partial activation of antithrombin against the clotting cascade, i.e., inhibition of the thrombotic factor, Factor Xa [4, 9]. About six additional specific disaccharides, adjacent to but different in structural detail from the major binding sequence, are required to produce the full heparin-activation of antithrombin function against the serpins of the clotting cascade (i.e., including thrombin). The anticoagulantly active heparin molecules, like the other heparin chains in the bulk preparation ("heparins"), vary in mass up to $\sim 22\,000$, the specificity for full activation of antithrombin residing in chains of $\geqslant \sim 6300$. Despite having very similar mass range, primary structure and anionic density to those of anticoagulant-heparin, a large majority of the heparins in the bulk preparation lack the capacity to activate antithrombin.

Heparins and heparan sulfates have now become more widely appreciated as being important modulators of many protein and cell membrane functions, including normal and disease processes in humans, e.g., normal and malignant cell growth (cytokines, cell signalling, angiogenisis, metastasis), lymphocyte homing, scrapie resistence and viral infectivity (including inhibition of the binding of the human immunodeficiency virus (HIV-1) to its target CD4 cell), as well as in the complement and coagulation cascades [9–29]. The molecular bases of these many functions remain largely unclear. It is likely, however, that certain specificity in structure, as described for anticoagulantly active heparin, may be involved. We have described a possible fundamental structural pattern for heparins and speculated that a unique difference in detail within this pattern might be associated specifically with each of the functions ascribed to the bulk heparin [30].

Heparin was found to be a potent inhibitor of the *in vitro* infectiousness of HIV-1 in the late 1980s [18–20] and some studies were undertaken to develop an agent against the acquired immune deficiency syndrome (AIDS), bearing in mind that the high anticoagulant action of the heterogeneous mixture precluded its direct use. In various studies, the inhibition was dose dependent and the 50% effective dose of the heparin inhibition of HIV-1 ranged from > 1 to $< 10\ \mu g\,ml^{-1}$. In an early study, this capacity appeared to be specific to the heparin structure among other sulfated glycosaminoglycans which were inactive (e.g., dermatan sulfate) [21]. Enzymatic fragmentation of heparin, however, showed a loss of antiviral capacity below a mass of ~ 5700, but failed to produce separation of the anti-HIV-1 potency from anticoagulantly active constituents. Recently, heparin and a pharmaceutical preparation of heterogeneous low molecular weight heparin (LMW heparin, average mass ~ 5200) were studied to compare their relative anti-HIV-1 and anticoagulation properties [22]. LMW heparin retained anti-HIV-1 capacity, but only a limited separation of antiviral activity from the anticoagulantly active heparin of either preparation was obtained. Comprehensive studies, however, which would be required to clarify structure-function relations of the anti-HIV-1 capacities of heparins having different size or functions, have been lacking.

A strategy to develop anticoagulant heparin-mimetic agents by chemical sulfation of various neutral biological polysaccharides was undertaken about three decades ago and a sulfated xylan, SP54™, for example, emerged as a major antithrombotic pharmaceutical. This heparin-mimetic comprises a heterogeneous mixture of sulfated oligoxylans (also called pentosan polysulfate) [31, review]. It has now been found to mimic the actions of heparins in most of the above systems *in vitro* [11, 18, 26, 28, 29, 32–35]. It is of note that currently its use in clinical practice other than protection from thromboembolism is expanding, e.g., against interstitial cystitis and radiation-induced proctitis. The sulfated oligoxylans, like heparins, inhibit both the direct entry cytopathic effect and the syncytium-forming, infective cell–cell fusion produced by HIV-1, and as with heparin the structure/function relations of their antiviral capacities have not been elucidated.

The deadly results of HIV infection became known about 1981 and AIDS caused by this infection presently remains a major national and international health threat, despite intensive international research towards prevention and a lasting cure. The role that endogenous sulfated polysaccharides might play in the natural history of AIDS is unknown. Clinical trials of various chemically sulfated polysaccharide products against AIDS, Kaposi's sarcoma, and cancers [23, 36–39], however, have been discordant with the expectations derived from the *in vitro* experiments. Considering the anticoagulant and/or other side effects possible when using such ill-defined mixtures of sulfated oligosaccharides *in vivo*, this might not be unexpected. Because of the importance of developing new and inexpensive modes of therapy against such diseases, as well as elucidating the molecular basis of the inhibition, the failure to exploit the potential of the anti-HIV and anti-cancer (and possibly other) actions of sulfated oligosaccharides needs to be examined carefully.

In pursuit of this, we addressed a central question concerning the potential for *in vivo* effectiveness of sulfated oligosaccharides against HIV-1, that is, whether the strong antiviral capacity of the mixtures was derived from specific molecular components or whether the inhibition was

non-speicific. In particular, would isolated SP54™ components display a degree of specificity by exhibiting differential antiviral potencies? Numerous Components were isolated and found to display differential potencies against the cytotoxic and the syncytium-forming infectivity of HIV-1 in several human CD4 cell lines in culture. Preliminary reports of parts of this work were given at the XIth International Symposium on Glycoconjugates [40] and at the 21st Annual Meeting of the Society for Complex Carbohydrates [41].

Materials and methods

Materials

Polyacrylamide gels were obtained from BioRad (USA), ammonium bicarbonate from Mallinkrodt (USA), methylene blue (MB) from Chroma Gesellschaft (Roboz Surgical Instruments Co., USA), D-glucuronic acid from Calbiochem (USA). Chemical reagents were reagent or analytical grade and all aqueous solutions were made using doubly glass-distilled water (referred to as water in following text). Chemical analyses were obtained from Galbraith Laboratories, Inc., USA.

Oligo- and polysaccharides

SP54™ (an antithrombotic pharmaceutical) was a gift from Dr. Dominique Scholz (bene-Arzneimittel, GmbH, Munich). SP54 is a mixture of sulfated 1–4 β D-oligoxylans produced by chemical sulfation of deciduous wood xylan (beechwood). A general structure representing such oligosaccharides is illustrated in Figure 1 [42]. Sulfation of a native beechwood xylan having an average degree of polymerization of ~ 70 would be expected to yield a sulfated polysaccharide averaging $\sim 24{,}000$ in mass. SP54, however, is characterized by the supplier as having an average molecular weight of 4000 to 6000, indicating that a general hydrolytic depolymerization of the polysaccharide occurred during the sulfation procedures [31, 42, 43].

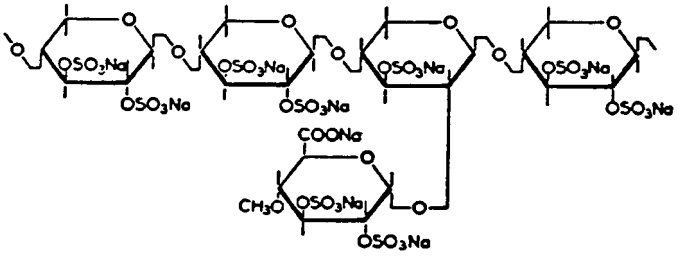

Figure 1. General structure of sulfated oligosaccharides derived from a deciduous wood xylan. Native beechwood xylan is composed of D-xylose linked linearly by β1–4 glycosidic bonds, with α-D glucuronic acid (almost all 4O-methylated) as monomeric branches randomly distributed on one in ten xylose moieties on average [42, 43]. The general structure reported for oligosaccharides produced by sulfation of the xylan is illustrated here by a sulfated pentasaccharide [42]. A linear tetramer of xylose in the pyranose ring conformation contains a sulfated, monomeric α1–2, 4OMe-D-GlcA branch on the 2-position of the second xylose from the reducing end. The sugars are sulfated at the C_2 and C_3 positions except for the 2-glucuronyl substituted xylose. Such moieties would impart α D-linkages along the β1-4 linked xylose chain.

Chromatographic molecular weight reference samples. The sulfated β-cyclodextrin, a highly sulfated cyclic heptaglucose having an average mass of ~ 2200 (sulfate content indicating 1.7 sulfates per glucose on the average), was a gift from Dr. Josef Pitha (NIA, Baltimore, MD). Beef lung heparan sulfate of molecular weight apparent = 30,000 and heparins of molecular weight apparent = 6600 and 22,000 were prepared as described [44]. λ-carrageenan was a previously characterized (45), highly sulfated polysaccharide from red seaweed [mass $> 10^6$] (Marine Colloids, USA); a 1–2 mg ml^{-1} solution in water was sheared before use by passage through a 31 gauge needle to reduce its average size and viscosity. Molecular-mass reference samples of sulfated oligoxylans were newly prepared having masses of 15,000, 9800, 7300, 5400, 4000, 3700, and 2700 (see below).

Biochemical methods

Liquid chromatography

The mixture of sulfated oligosaccharides was fractionated by gel permeation liquid chromatography through Bio-Gel P10 in 0.5 M ammonium bicarbonate in a column 196 cm × 0.6 cm, for 27 hr at a flow rate of 3 ml hr^{-1}. Ten mg in 100 µl of saline (supplied in 100 mg ml^{-1} ampules) was applied to the column, maintaining < 0.5 cm sample height during loading, and fractions of 0.855 or 0.80 ml were collected. The void volume was determined using λ-carrageenan prepared as above and the total elution volume was indicated by phenol red. Molecular weight chromatographic reference samples were 30,000 (heparan sulfate), 22,000 and 6600 (heparins), 2200 (sulfated β-cyclodextrin). Fractionations among different columns were reproducible, and on a given column consecutive runs were reproducible up to at least seven runs, after which there was a slight compression in the chromatograms towards the void. This could readily be taken into account in correlating the fractions.

Post-column assay

Measurement of concentration of the oligoxylan fractions on line by absorption or refractive index changes was not feasible because of the absence of a specific absorption band > 200 nm and the high salt concentration in the solvent, respectively. The eluting fractions were, therefore, monitored post-column on the basis of the amount of their metachromatic reactivity with the cationic dye, methylene blue [46], in a one-point spectrophotometric assay using the slope method [47]. Fractions were lyophilized for 36 h to remove water and ammonium bicarbonate, and redissolved slowly in water by first adding 200 µl over the sample and allowing the samples to remain undisturbed for several

hours at room temperature or overnight at 5–8 °C. Additional solvent was then added gradually with hand mixing to a final volume of one ml (200 µl or 500 µl total volume for fractions expected to be low in concentration) and the sample was then mixed vigorously on a vortex mixer.

Five or 10 µl of the solution (or an appropriate dilution) were added to 1 ml of a standardized methylene blue solution (11–12 nmol of positive charge per ml). The resulting induced hypochromism, measured at 663 nm as the difference between the optical densities (O.D.) of the free dye solution and that of the metachromatic solution, was processed by our computer program to calculate the µl of the fraction at the equivalence point, and hence the nmol of negative charge per µl of fraction (detection limit in the 1 ml assay = ~0.7 nmol of charge; the minimum concentration = ~30 nmol charge per ml (~4 µg ml^{-1})): i.e.,

$$\mu l \text{ of sample at equivalence point} = kS$$

where S, the slope = µl sample added/change in O.D.; and k, a constant, = O.D. of the free dye solution − O.D. of the solution of totally bound dye (= maximum change in O.D.).

The maximum hypochromism, and hence the total change in O.D., was weaker with the later-eluting fractions (similar to findings among the heparin poly- and oligosaccharides [48]). The k values for fractions in the various regions of the chromatogram were determined, therefore, and used accordingly. The amount of each fraction in the chromatogram was expressed as µg of the metachromatically active oligosaccharides per ml by multiplying µmoles of charge by the equivalent weight (weight per charge) of a disulfated xylose monomer, which = 146. Samples having an average charge density below 0.7 per sugar would be expected to produce metachromatic reactions that would be too weak to be quantitated by this method [46].

Preparation of sulfated oligosaccharide Components

The above fractions were relyophilized. Corresponding dried fractions from five fractionations were dissolved in water as above and combined in accordance with the chromatograms to obtain 15 oligosaccharide Components (see Results). These were relyophilized to remove any remaining ammonium bicarbonate and then characterized on the basis of dry weight and relative yield. Spectrophotometric titration of the negative charges of a weighed aliquot yielded the weight per mol of charge which equals the equivalent weight on the average of the Component.

Preparation of bioassay samples

A weighed amount of each Component was dissolved slowly in water as above to a final concentration of 1 to 3 mg ml^{-1} for bioassay. (Some samples were highly electrostatic.) Aliquots of 10 µl were added to 100 µl of water for quantitative spectrophotometric titration [46]. The remainder was sterilized by filtration through a 4 mm diameter luer-type 0.22 mm filter (Millipore Products, USA). A 10 µl aliquot was taken under sterile conditions after filtration and added to 100 µl of water for analysis as above. Comparison of the titrations before and after filtration showed no change in concentration upon filtration for all of the Components.

The spectrophotometric titration also determined the maximum metachromatic reaction produced in methylene blue by each Component. This optical parameter provides a characteristic of many polyanions and is expressed as the minimum extinction coefficient at the α absorption band, 663 nm ($E_{\min \alpha}$).

Biological assays

Inhibition of cytotoxic infectivity of HIV-1 in vitro

The capacity of the purified Components to inhibit the cytotoxic infectivity of HIV-1 was measured at the Laboratory of Drug Discovery Research and Development in the National Cancer Institute, using their microculture colorimetric method with a susceptible human CD4 cell line (CEM-IW) [49]: a metabolic, reductive conversion of a colorless tetrazolium reagent to a soluble orange formazan is produced by viable, living CEM-IW cells but not by killed cells. The assay is designed for assaying the dose-response curves of samples with comparison among samples within a group and between groups.

Cells were cultured under four conditions: uninfected; infected; uninfected/treated; and infected/treated. In the treated cultures, concentrations (in µg ml^{-1} dose) of the sulfated xylan Component was varied over a range of five or six logarithmic units. After seven days, the tetrazolium reagent was added to the cell wells and the number of viable cells at each dose was determined from the optical density at 450 nm after 4 h of incubation. The viral cytopathic effect on infected cells usually destroyed a maximum of about 90% ± 5% of the uninfected cells during that time. The uninfected culture was paired with the infected culture to delineate the 100% protection reference (taken at 0% viral cell-killing) and the 0% protection reference (taking the maximal cytopathic effect level as 100% cell-killing). The 50% protection level thus delineated is required for the computation of the 50% effective (inhibitory) concentration of oligosaccharide (EC_{50}) from the dose-response curve.

Two experimental dose response curves were obtained in the treated cultures: (1) The percent of cells in the infected/treated cultures relative to the uninfected culture was plotted against the dose of oligosaccharide to yield the EC_{50} by computation from the 0% and 100% protection reference lines; and (2) the percent of cells in the uninfected/treated cultures relative to the uninfected culture was plotted against the dose to reveal any change in the percent of uninfected cells that might have derived from the Component alone at the same dose range (e.g., cytotoxicity or other effects). Assays were performed in duplicate and then subsequently repeated in duplicate. Because of the

normalization between 0% and 100% cell-killing in these assays, comparisons could be made between different groups of assays.

Inhibition of the syncytium-forming infectivity of HIV-1 in vitro

Another series of Components was prepared from a second lot of SP54. Capacity to inhibit the syncytium-forming infectivity of HIV-1 was measured *in vitro* by a quantitative microliter well assay established by Peter L. Nara at the Frederick Cancer Research and Development Center, National Cancer Institute, using a human-derived CD4 lymphocyte line other than that above, i.e., CEM-SS cells [50]. Briefly: Virus production was maintained in a chronically infected human T-lymphocyte cell line, H9. Viral infectivity expressed in syncytium-forming units (SFU) and viral titers was determined before use. Chronically-infected cells of known amount of SFU were added to 50,000 uninfected CEM-SS target cells in microliter wells in the absence of and presence of increasing concentration of sulfated xylan Component, and the total number of syncytia formed per well in 24 h was counted. Dose-response curves were generated as percent of syncytia formed in the presence of the Component relative to that formed by the untreated cocultures. This series of Components was also tested for inhibition of the cytotoxic infectivity of HIV-1 in the same assay as above, except for the use of the CEM-SS cells.

Molecular mass markers

The reference heparan sulfate and heparins of mass $\geqslant 6500$ were used as chromatographic markers to indicate the apparent molecular weight range of the sulfated oligoxylans on the relatively high mass side of the chromatogram, but smaller heparin oligosaccharides of known mass would not be expected to be appropriate standards [8]. The relatively greater sulfate charge per mass in the smaller oligoxylans would likely result in relatively higher elution volumes than such standards. The sulfated β-cyclodextrin gave the position of a highly sulfated cyclic heptamer. No series of sulfated oligoxylans of known mass were available, however, to serve as suitable reference markers in other regions of the chromatogram. To this end, we prepared a series of marker-oligoxylans by a subsequent purification of various Components. These were monodansylated at the reducing end by an adaptation of the Avigad reaction [51], to produce derivatives with an absorption band above 300 nm (Spitsin SV and Stone AL, unpublished data).

Measurement of molecular mass of reference sulfated oligoxylans

To determine the mass of the above marker oligosaccharides, and thereby provide an estimate of the mass of the Components at various elution regions of this chromatographic separation, the derivatized Components were analyzed by equilibrium ultracentrifugation in the Beckman Model E ultracentrifuge equipped with absorption optics and a computer data acquisition system scanning at the absorption maximum of the dansyl derivatives, 335 nm [52]. Samples were analyzed at 20 °C, at appropriately high salt (0.5 M NaCl) and low concentration to minimize polyanion effects, and at an optical density of 0.2–0.4. The speed was 24 000 RPM for estimated mass $\geqslant 7000$ or 32 000 RPM for mass estimated at < 7000. Solutions were made by adding $\sim 200\,\mu l$ of water to the sample and allowing the sample to dissolve undisturbed for several hours at room temperature or overnight at 5–8 °C. The solution was then gently agitated manually several times and an amount of water to give the required optical density was added slowly and the mixture was stirred. The aqueous solution was brought to 0.5 M NaCl by the addition of 3 M NaCl.

The value of the compositional partial specific volume ($\bar{\nu}$) of the sulfated oligosaccharides was calculated using Traube's values for the partial molar volumes of C, H, and O as described by Zamyatnin [53] and values for inulin and sulfuric acid as given by Durchschlag [54] (i.e., by subtracting appropriate contributions from C, H, and O of inulin to obtain that of xylose, and adding the contribution from the sulfates). The value thus obtained for the compositional partial specific volume of the disulfated xylose moieties was 0.475. Consideration of the effect of the average GlcA content of xylan (one branch in ten xyloses) on the calculated compositional partial specific volume gave a similar value. This value was similar to the experimental values for heparin, 0.45 and 0.47 in water and 0.5 M NaCl, respectively [55], and 0.46 in 0.15 M NaCl [56], and yielded $1 - \bar{\nu}\rho = 0.5162$, where ρ is the density of the solvent. The sedimentation data were fitted to a mathematical model that describes the concentration distribution of a homogeneous ideal solute to yield an observed weight-average molecular mass. Computations were made using the MLAB program software [57].

Calculation of corrected molecular mass of sulfated oligosaccharides

Determination of the mass of charged molecules, such as the polyanionic sulfated xylans, by ultracentrifugation analysis yields an observed mass which is lower than the actual mass because the polyanionic charge on such polymers affects their sedimentation in the NaCl solvent, and this effect would be dependent on the mass. An equation by Williams *et al.* [58], however, accounted for this effect and was modified by Jordan *et al.* [56] for the determination of the molecular weight of heparins. Since the present studies utilized absorption optics, the latter equation was further simplified by removal of a term which corrected for changes in refractive index of the solvent. The resulting equation relating the observed mass to the actual mass was

$$\text{Equation 1.} \qquad M_o = M\left[1 - \left(\frac{ZM_s(1 - \bar{\nu}_s\rho)}{2M(1 - \bar{\nu}\rho)}\right)\right]$$

where M_o = observed mass; M = actual mass of the Component; M_s, the mass of NaCl, = 58; $\bar{v}_s$, the partial specific volume of NaCl, = 0.282; $\bar{v}$, the partial specific volume of the Component, = 0.475; and ρ, the density of the solvent, = 1.0185. The value of Z, which is the effective charge on the sulfated oligosaccharide, was calculated by dividing M by the equivalent weight of a disulfated xylan (Z = M/146). Equation 1 thus yielded the relationship in

$$\text{Equation 2.} \qquad M = M_o/0.726.$$

Because polyanions variably tend to hold solvent cations (gegen ions) close to their surfaces, the effective polyanionic charge might be less than the total number of charges and then Z would be smaller. In such case, M might be overestimated when M_o is corrected by equation 2. To evaluate such a possible overestimation, we calculated that if as much as 20% of the charges did not contribute to the effective charge, M would be overestimated by about 10%.

Space-filling model of a sulfated oligoxylan and uronic acid content of Components

The effect of the α-*D* linkage of the glucuronic acid moiety on its geometry relative to the 1,4-*β* linked sugar chain and the sulfate groups on the neighboring xyloses was examined by building a Courtauld-Kolton space-filling atomic model (Harvard Instrument Co., USA) of a sulfated xylan octasaccharide containing a 4-OMe-GlcA substituent on the central xylose. Color photographs of the model were taken at several positions about the axis to illustrate these relationships.

The GlcA content of fractions and Components was measured by a colorimetric method [59, 60], as modified by Bystricky and Szu [61]. The carboxyl group was activated by water soluble ethyl-dimethyl-aminopropyl-carbodiimide (EDC) and coupled with 2 ortho-nitrophenyl-hydrazide (o-NPH) to yield purple products that were quantitated in the μg range against GlcA as the standard. Details of application of this method to the measurement of carboxyl moieties of highly sulfated oligosaccharides will be the subject of a separate report.

Results

Native, unsulfated beechwood xylan is composed of a linear chain of pyranose xylose rings ($n = \sim 70$–100) linked by β1,4 glycosidic bonds, with monomeric 4-OMe α1–2 linked GlcA branches that are thought to occur randomly on one in ten xyloses on the average [43]. Sulfation of a native xylan that has an average degree of polymerization of ~70 would be expected to yield a sulfated polysaccharide averaging about 24,000 in mass. SP54™, an antithrombotic pharmaceutical produced by a patented chemical sulfation of this xylan, however, is characterized by the provider to be a mixture of sulfated oligoxylans having an average molecular mass of 4000 to 6000. This has been attributed to non-specific hydrolytic depolymerization during the sulfation process [31, 42, 43]. Thus, SP54, has been a poorly defined mixture of oligosaccharides that could differ in size, primary structure, and/or degree of sulfation. The present studies have started to define constituents of this heparin-mimetic mixture by isolating and characterizing many chromatographic Components and by studying their structure-function relationships.

Preparation of sulfated oligosaccharide Components of the mixture

Components were obtained by fractionation of the mixture through BioRad P-10 gel in 0.5 M ammonium bicarbonate as detailed in Methods. The amount of oligosaccharide in each fraction was measured after fractions were collected, lyophilized and redissolved in water, using the one point metachromatic assay [47] to give the μg of metachromatically reactive sulfated oligoxylan, as described in Methods. The results of a series of many fractionations were reproducible on the same or on duplicate columns, yielding chromatograms which exhibited numerous unresolved peaks (Figure 2) over a broad range of elution volumes.

After relyophilization, fractions from each chromatographic separation were selected into groups which divided the unresolved peaks of the sulfated oligosaccharide mixture into fifteen Components. The elution-volume boundaries of these groups are delineated by the vertical lines on the chromatogram (Figure 2). Corresponding groups of fractions from five consecutive fractionations were redissolved and combined to yield the final Components in this series. The Components were numbered arbitrarily in sequence, as shown in Figure 2. Those that comprised relatively more fractions (and/or multiple peaks) were assigned dual numbers.

The dried Components were weighed, yielding a recovery of ~115%. The relative amount of the Component in the original mixture, expressed as percent of the total dry weight, is shown in Table 1, column 2. The yield obtained by the measured dry weight accounts for all of the content of each Component in this series, while the μg/ml plotted in the chromatogram (Figure 2) was based upon the metachromatically reactive oligosaccharides and calculated as an average disulfated sugar content (as described in Methods). The amount of Component based on dry weight corresponded with the amount calculated from metachromatically reactive oligosaccharides, for most of the Components. This would be expected of oligoxylans that were highly sulfated on the average. Two Components that eluted on the relatively low mass side of the chromatogram, however, i.e., 15/16 and 19, yield a much greater dry weight than expected from the amount of metachromatically reactive sulfated oligosaccharide contained in those Components (Figure 2), (see further below).

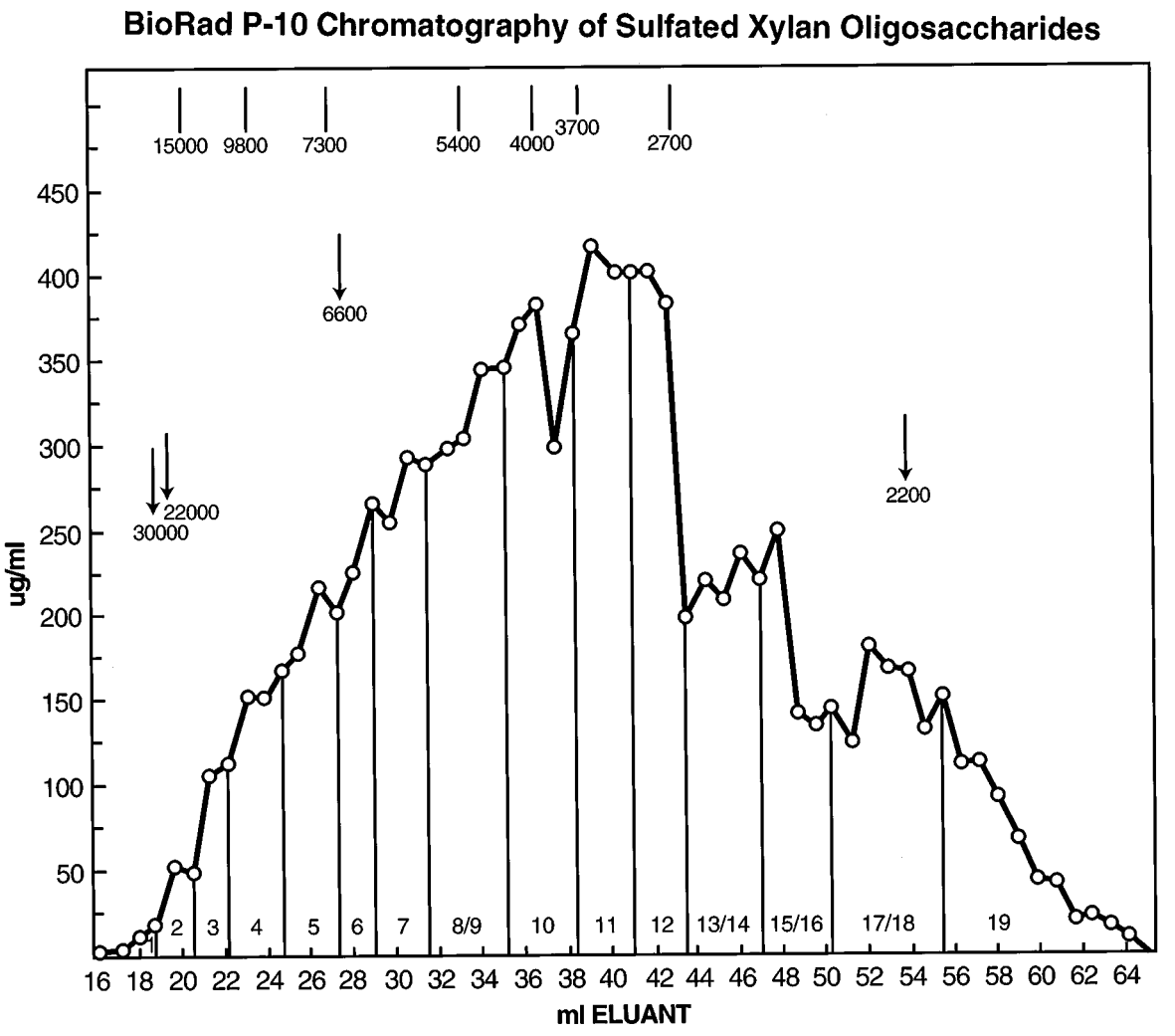

Figure 2. BioRad P-10 chromatography of sulfated xylan oligosaccharides. Ordinate: –○–, μg of metachromatically reactive oligosaccharide per ml. Abscissa: ml of elution volume through BioRad P-10 in ammonium bicarbonate (0.6 × 196 cm). Perpendicular lines along the elution volume delineate the boundaries of fractions which were combined to yield the various isolated Components of sulfated xylan. The Components are arbitrarily numbered consecutively in order of elution. Descending arrows above the chromatogram mark the elution positions of the chromatographic standards: 30,000 MW_{app} fraction of beef lung heparan sulfate, 22,000 and 6600 MW_{app} fractions of pig mucosal heparin, and sulfated β-cyclodextrin, 2200 in average mass. The bars at the top of the figure give the elution positions of sulfated oligoxylan mass markers. These were prepared from Components that were isolated by the same BioRad P-10 chromatography as above, using monodansylation and then ultracentrifugal analysis of the oligosaccharides to obtain their masses (shown under the bars).

Molecular mass of Components relative to heparin and sulfated oligoxylan markers

The descending arrows on the chromatogram (Figure 2) mark the elution positions of four chromatographic standards that show the molecular weight apparent across the chromatogram. These indicate that the range of molecular mass among the fractions was broad, approximately 20,000 to < 2000, but no series of sulfated oligoxylan standards was available to serve as the appropriate mass markers throughout the fractionation. We prepared such references as described in Methods. Briefly, the mono-substituted dansyl derivatives of additionally isolated Components were subjected to conventional sedimentation-equilibrium ultracentrifugal analysis to measure their weight-average molecular mass. The elution positions of these markers are shown by the vertical bars at the top of the chromatogram, with the corresponding mass given under each bar (Figure 2).

The concentration distribution of the marker samples in the sedimentation analyses could not be distinguished from that of a homogeneous ideal solute, with two exceptions, the 4000 and 2700 samples. For these samples, calculation of the mass using a two component system in this analysis readily yielded a good fit to the theoretical curve and showed that the failure to fit the curve for a single component system was due to a small amount of spurious grossly aggregated

Table 1. Characteristics of Components of the first sulfated oligoxylan series

Elution region	*% Yield of dry weight*	*Equivalent*[1] *weight*	*Extinction*[2] *coefficient at min α*
1	0.4		
2	1		
3	1.4		6000
4	2.4		6000
5	4.5	156	6800
6	3.1	145	6400
7	6.4	149	6000
8/9	9.0	139	8900
10	9.7	156	9000
11	6.1		13000
12	7.0	177	13000
13/14	7.6	208	~ 14000
15/16[3]	28	1170	
17/18	3.0	133	18500
19	11	1080	23500

[1] Equivalent weight = dry weight per mol charge titrated by methylene blue, i.e., $\mu g\,ml^{-1}$ per μmol negative $charge^{-1}\,ml^{-1}$. Weight per mol of charge of disulfated xylose = 146.

[2] The extinction coefficient (at 663 nm) at the point of maximum hypochromism in the methylene blue titration of Components.

[3] The average anionic density of this Component was insufficient to quantitate by this titration.

material, about 11% and 7%, respectively. There was no indication of dimerization or oligomerization of molecules in any of the sample solutions. This relatively sharp distribution of mass of the standards seen by ultracentrifugal analyses was supported by examination of the molecular distributions of a number of the underivatized Components by HPLC using the Waters Maxima 820 GPC chromatography software system. The Mw/Mn values ranged 1.02 to 1.16 from the high to low mass (Stone AL and Orvisky EO, unpublished data).

These markers (Figure 2) indicate that the major metachromatically reactive peaks of the fractionation fell between ~3000 and 5500 in mass, which is similar to the 4000–6000 stated by the provider to be the apparent molecular weight of the mixture. Components of ~22,000 to 6000 in mass, however, comprised about 15% of the mixture. Components 8/9 and 10, comprising ~19%, eluted in the region of about 5000 to 3900 in mass, and Component 13/14, ~8% of the total, in the region of 2700 in mass.

Polyanionic characteristics of sulfated xylan Components

Equivalent weight

Aliquots of the dried Components were weighed and dissolved in water as above to yield solutions of known concentrations in $\mu g\,ml^{-1}$. The nanomoles of anionic charge per ml of these solutions were determined by quantitative spectrophotometric titration with methylene blue. Given the known $\mu g\,ml^{-1}$ and μmol of negative charge per ml of the Component, an average equivalent weight (weight per molcharge) of the oligosaccharides was calculated for the various Components in this series (Table 1, column 3). The equivalent weight is an indication of the average anionic density of the Component and may be compared with that of disulfated xylose (146). Table 1 shows that the equivalent weights of most of the Components, comprising ~60% of the sulfated oligoxylans, ranged between 133 and 208. The data show that the weight of these Components is largely accounted for by metachromatically reactive oligoxylans that have a relatively high average degree of sulfation. Moreover, this high average degree of sulfation was found in Components prepared from the relatively low mass region of the chromatogram as well as those prepared from the high mass and major mass regions.

Component 15/16 (more than a quarter of the yield), however, displayed a much larger equivalent weight. This caused artificially low values of the "$\mu g\,ml^{-1}$" calculated for the fractions in the 15/16 region of the chromatogram (Figure 2). It was very weakly metachromatic (only ~15% gave a measurable degree of metachromasy). Its relatively high ash residue suggested that in addition to low sulfate, salts from the production process (e.g., Ba^{++}, Ca^{++} or Na^{+}) might be present in this Component. Component 19, which eluted at the end of the chromatographic fractionation similarly appeared to comprise products relatively low in average sulfate content.

Strength of the metachromatic reactivity

Since the extent of hypochromism in the α absorption band of methylene blue ($E_{min\,\alpha}$, Table 1, column 4) is correlated with the strength of dye-dye coupling in methylene blue metachromasy [62], the quantitative spectrophotometric titration also yielded the strength of the metachromasy produced by the reactions between methylene blue and the various Components. The strongest ligand coupling (lowest $E_{min\,\alpha}$) was observed with the Components in the early eluting region (up to a volume of about 31 ml in the mass region $\geqslant 6000$). $E_{min\,\alpha}$ was higher for Component 8/9 and 10, and rose sharply thereafter. Strength of dye coupling would depend upon the effective anionic density (density and geometry of charge) and tend to decrease with the shorter polyanion chains as the number of internal sugars, which impart polyanionic characteristics, decreases. Significant decrease in anionic density would also result in a reduction in the strength of metachromatic reactions. As with those of the heparin molecular weight components [48], these $E_{min\,\alpha}$s appear to be characteristically associated with Components from a particular elution region.

Inhibition of the *in vitro* cytotoxic infectivity of HIV-1 by Components

To study the anti-HIV-1 potencies of the various Components of the sulfated xylan, weighed aliquots of each of twelve Components were dissolved in water as above, sterile-filtered and tested with comparison by the tetrazolium assay [49] for their inhibition of the cytotoxicity of HIV-1 (Methods). Quantitative titration of the bioassay samples before and after 0.22 mm millipore filtration demonstrated that no change in the concentration was caused by this sterilization procedure (data not shown). The 50% effective (inhibitory) concentration of the sterile-filtered Components in $\mu g\,ml^{-1}$ (EC_{50}) was computed from dose-response curves such as those in Figure 3 (left panel), which were obtained as described in Methods. Dose-reponse curves of Components over the range of the chromatogram (Figure 2) are illustrated by those of Components 5 (◆) (relatively high mass) and Component 17/18 (●) (lowest mass assayed). The dose-response curves of Components 11 (■) and 13/14 (▲) are also shown.

The top line, –·–·–, delineates 100% of the viable cells in uninfected cultures (left ordinate), which defines the 100% protection reference line (right ordinate). The bottom line, ····, delineates the % of viable cells in infected/untreated cultures relative to those in the uninfected cultures after maximal cell-killing by HIV-1 (left ordinate) and defines the 0% protection reference line (right ordinate). The 50% protection line, –·–·–, for a given dose-response curve (filled symbols) was derived from the above two reference lines and used to compute the EC_{50}.

The EC_{50}s thus obtained for the twelve Components are plotted (Figure 3, right panel) on a logarithmic scale against their respective elution positions. The elution positions are expressed as the fraction of the total elution volume, a descriptive parameter of the Component, chosen to facilitate comparison of results obtained from different preparations. Comparison of the data in Figure 3 (right) shows that the structure(s) required for high capacity against HIV-1 fall in the elution volume-fraction region < 0.3 (average mass of Components $\geqslant \sim 5500$), and that the minimum average size required for this high potency function is seen around an elution volume-fraction of 0.30–0.33. Thereafter, a sharp fall in potency occurs in the regions of larger elution volume-fractions, but with the notable exception of Component 13/14 which displays a relatively high potency as well as the elution volume-fraction of ~ 0.59. The dose-response curves of Components 11 and 13/14, compared in Figure 3 (left panel), further illustrate this biphasic dependency of inhibitory capacity of the Components on the average molecular mass (average $EC_{50} = 15$ and $3.6\,\mu g\,ml^{-1}$, respectively). It is also noteworthy that Component 17/18, which has a relatively high average anionic density, similar to that of highly active Components (Table 1), is inactive. Thus, the isolated Components in this initial study have revealed that high anti-HIV-1 activity is associated with structure(s) residing in molecules both relatively high and low in size, and that a high degree of sulfation per se is not sufficient to endow anti-HIV-1 potency.

Corresponding dose response curves for Components in uninfected/treated cell cultures relative to uninfected cultures alone (left panel, left ordinate) are shown by open symbols. These curves would reveal any cytotoxic or other effects due to the Components alone. The data overall indicates little effect on the cells by the Components alone until a concentration of $\log_{10} \geqslant 2.5$, where the percents of control cells begin to decline. This value is $\geqslant$ three logarithmic units from the EC_{50}s of the highly active Components.

Considering the data in Figures 2 and 3 overall, three regions of molecular size may be defined regarding the observed differential anti-HIV-1 cytotoxicity potencies of the Components of the sulfated xylan mixture in this series of fractionations: (1) a highly active region (EC_{50} of 0.5 to $0.8\,\mu g\,ml^{-1}$), $\geqslant \sim 5500$ in average mass, (2) a region of minimum-sized highly active structures, ~ 4500–5000 in average mass (containing as well some oligosaccharides of low potency) and (3) a region of average mass ~ 2700 and below, containing a Component of high activity among mainly inactive oligosaccharides. Thus, at least two sulfated xylan structures might be heparin-mimetic against-HIV-1, one (or both) in regions (1) and (2), the second eluting in the average mass region of a nonosaccharide, which would be smaller than any previously recognized active component of the mixture. The differential potencies displayed by the various Components indicated that the inhibition of HIV-1 by the sulfated xylan was governed by a degree of molecular specificity and not due solely to a non-specific high charge density.

Inhibition of syncytium-forming infectivity of HIV-1 in human cell cultures

The infective fusion of multiple uninfected CD4-lymphocytes by a single HIV-1-infected cell is manifest in AIDS by the formation of syncytia ('giant cells'). Given the differential nature of the capacity of the sulfated oligoxylans to inhibit the cytopathic effect of HIV-1, it was desirable to study also their capacity to protect against the syncytium-forming infectivity of the virus.

Preparation

To this end another series of Components was prepared using the same methodology as above. The elution boundaries of these Components were selected to be narrower than those in the first series, and the number of runs combined was 14. Figure 4A shows an example of this chromatography and the boundaries defining the 24 Components. The shaded areas correspond with the elution volumes of Components 8/9 and 13/14 in the first series (Figure 2) and thus highlight the further fractionation of regions 8/9 and 13/14 by isolating an additional three and

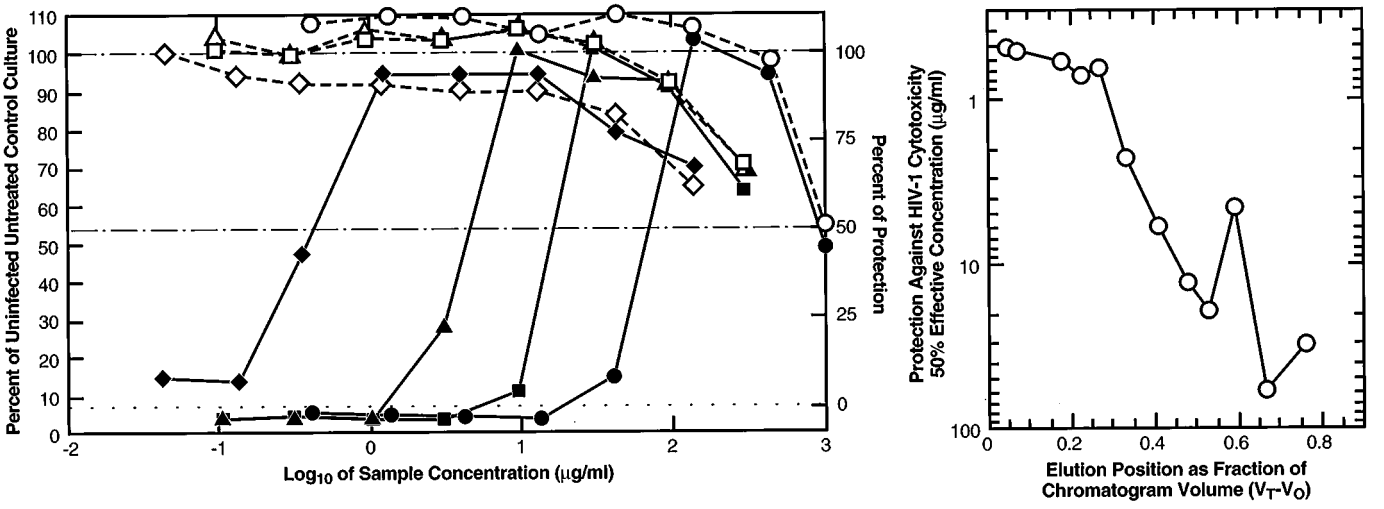

Figure 3. Differential inhibition of the cytotoxic infectivity of HIV-1 in human-derived lymphocytes by various Components of sulfated xylan. *Left Panel*. Dose-response curves in the tetrazolium cytotoxicity assay of representative Components: Top line, –·–·–, 100% of the cells in the uninfected cultures (left ordinate). This equals 0% cell-killing and delineates the 100% protection reference line (right ordinate). Bottom line, ····, % of viable cells in infected/treated cultures at maximal HIV-1 cytopathic effect (10 ± 5%) relative to uninfected cultures. This is taken to equal 100% cell-killing and delineates the 0% protection reference line (right ordinate). –·–·–, 50% protection line derived from the 100% and 0% reference lines and used to compute the 50% effective (inhibitory) concentration (EC_{50}). The dose response relative to the % of cells in uninfected cultures is plotted against the dose (log_{10} scale) of Component in the infected cultures: —◆—, Component 5, —▲—, Component 13/14, —■—, Component 11, and —●—, Component 17/18, to yield the EC_{50}s in $\mu g\,ml^{-1}$. The corresponding dose response in uninfected cultures (Component without HIV-1) is also plotted against the dose, ----, open symbols. *Right Panel*: EC_{50}s of Components 2, 3, 5, 6, 7, 8/9, 10, 11, 12, 13/14, 15/16, and 17/18 are plotted on a log_{10} scale against their elution volume-fraction, $V_e - V_o/V_t - V_o$, where V_e = elution volume; V_o = void volume; V_t = total volume.

four Components, respectively, from within those elution volumes. The distribution of the percent of total yield of the fractions across the chromatogram reproduced in general that of the first series (data not shown), and the $E_{min\alpha}$s (legend Figure 4) again seem to be characteristically associated with the given elution volume-fractions.

The difference in the sharpness of the decline of the $\mu g\,ml^{-1}$ fraction between this fractionation and the first chromatography, seen at the last part of the chromatograms, may be attributed to a difference between the two batch lots of SP54 as well as to possible technical variation in the properties of the gel. In addition, the large proportion of relatively small products having low metachromatic reactivity, which eluted in this region, might have affected the average metachromatic reactivity of some of the fractions in the two series differently.

Protection from infective fusion

The capacity of the Components to inhibit the syncytium-forming infectivity of HIV-1 was measured *in vitro* by a quantitative assay which employed a second human-derived CD4-lymphocyte (CEM-SS) as the target cell (Methods). The percent of syncytia formed in the presence, relative to that in the absence, of Component at 24 h was plotted against the log_{10} of the concentration to yield the dose-response curves of the various Components (data not shown). The 50% effective concentrations were derived from the dose response curves and plotted against the elution volume-fractions of the Components (Figure 4B), revealing that the sulfated xylan Components displayed differential potencies against the syncytium-forming infectivity of HIV-1 as well as in the inhibition of the cytotoxic infectivity

Figure 4. Differential inhibition of the syncytium-forming infectivity of HIV-1 by various Components of sulfated xylan. *Panel A*. BioRad P-10 chromatography of sulfated xylan oligosaccharides. Chromatographic conditions and the chromatogram are similar to that described in Figure 2, with the exception that the perpendicular lines mark narrower boundaries of fractions, yielding 24 (instead of 15) isolated Components that are arbitrarily numbered in order of increasing elution volume. The two shaded areas comprise Components that correspond with Components 8/9 and 13/14 in Figure 2. *Panel B*. The 50% effective (inhibitory) doses of Components against syncytium formation. EC_{50}s determined from dose-response curves relative to the percent of syncytium forming units (SFU) in untreated cocultures, –○–, are plotted against the elution volume-fraction of the Components as defined in Figure 3. The corresponding $E_{min\,\alpha}$ of Components 2 to 18 across the elution region are: 5200, 5800, 6000, 6900, 7000, 7000, 7600, 8100, 11,000, 11,000, 12,500, 13,800, 15,000, 18,600, 32,000, 28,000, 29,000, and 32,000, respectively.

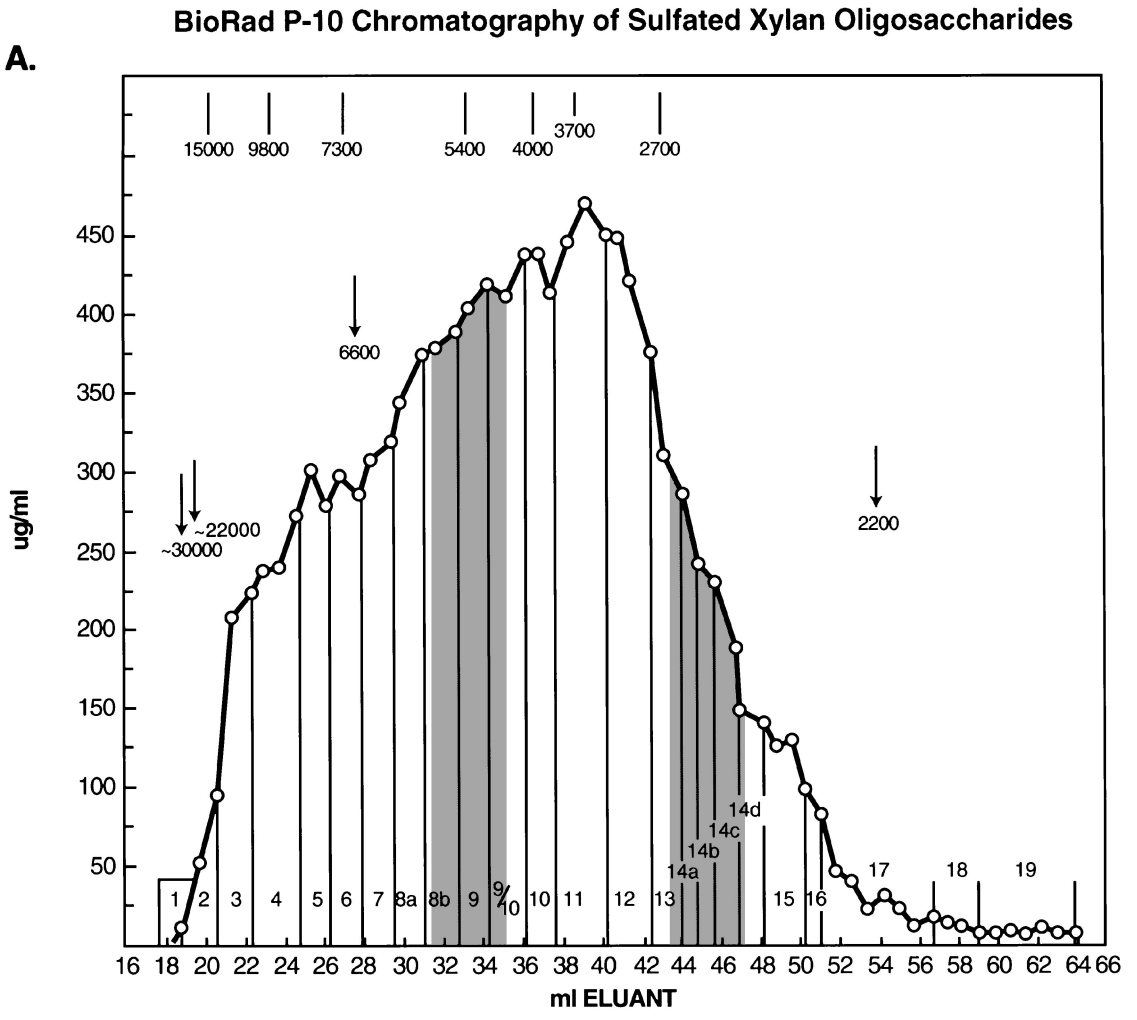
BioRad P-10 Chromatography of Sulfated Xylan Oligosaccharides
A.
15000
9800
7300
5400
4000
3700
2700
6600
~22000
~30000
2200
ug/ml
ml ELUANT
1
2
3
4
5
6
7
8a
8b
9
9/10
10
11
12
13
14a
14b
14c
14d
15
16
17
18
19

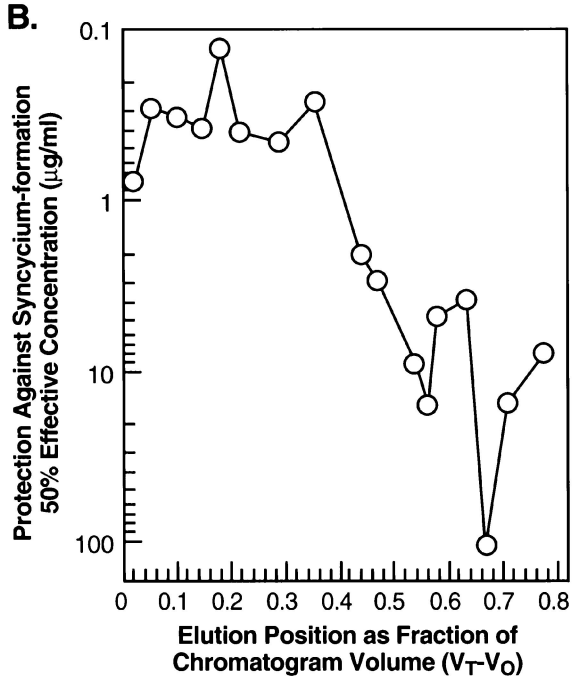
B.
Protection Against Syncycium-formation
50% Effective Concentration (μg/ml)
Elution Position as Fraction of
Chromatogram Volume (V_T-V_O)

(Figure 3B). The minimum size for high activity against syncytia formation appears at an elution volume fraction of > 0.360 (Component 9/10), after which there is a fall in the potency with mass, with a possible exception at elution volume fraction about 0.609.

These Components were also assayed for their capacity to inhibit the cytotoxic infectivity of HIV-1 in the CEM-SS cultures (tetrazolium assay). The results confirmed the differential potencies described above (Figure 3). The EC_{50}s of the highly active Components in this series of isolations were 0.1–0.5 $\mu g\,ml^{-1}$, and the further fractionation in the region 8/9 (first series) elucidated that the fall in potency occurred at an elution volume-fraction of 0.33. As was noted in a preliminary report [63], the minimal average size of Component required for containing high-potency inhibition of cytotoxicity of HIV-1 appears to be larger (region ~ 5400 in mass) than that required to retain high potency against syncytium-formation (~ 4500). This would suggest that the sulfated xylan might act by different molecular mechanisms against the two direct effects of HIV-1 which kill immune cells.

Further studies on the structure-function relations of the sulfated xylan Components would depend upon application of methods for their additional purification and the development of an upscaled fractionation. In a study and report still in progress, the feasibility of additional purification by chromatographic means was indicated. Active and inactive molecules of Components in the 9/10 and 13/14 regions were further separable, e.g., Rechromatography through the P-10 system of a Component 9/10, which comprised the average minimum-size for high anti-syncytium-forming potency, displayed enrichment of potency from the unfractionated, $EC_{50} = 230\,ng\,ml^{-1}$ vs syncytium formation, to an $EC_{50} = 50$–$100\,ng\,ml^{-1}$ for fractions from the rising part of the peak of the subfractionation; relatively inactive molecules eluting in subsequent fractions showed increased values up to $2300\,ng\,ml^{-1}$.

Glucuronylxylose moieties of sulfated xylan oligosaccharides

Uronic acid content of sulfated oligoxylan components

The native xylan has as average of one 4-OMe-GlcA branch per ten xylose units [31, 42, 43]. This constituent of the sulfated xylan, however, has been largely disregarded by others to date, most likely because of its low average content. It was of interest to determine what the average ratio of GlcA to xylose was in the various Components. To this end we measured their GlcA content by applying the colorimetric reaction of activated carboxyl groups with o-nitrophenyl hydazine [59–61], using GlcA as standard. (The reaction between uronic acids and carbazole in sulfuric acid [66] was also applied.) Details of these experiments are the subject of a separate report (Melton DJ Henry AT and Stone AL, in preparation). We note here, however, that contrary to the percent GlcA expected when calculated on the basis of the average ratio of GlcA : Xyl in the native xylan (i.e., one trisulfated OMeGlcA-Xyl disaccharide + nine disulfated Xyl), which is 5.5% measured against a GlcA standard, many of the fractions gave values ranging up to two to three times higher. These data are the first to suggest that oligoxylans resulting from the sulfation process are relatively enriched in GlcA moieties. The enrichment in GlcA of these sulfated, partially depolymerized products produced during the sulfation process might be explained if the glucuronic acid branches hindered the hydrolysis of nearby glycosidic bonds, as was noted in an early paper on the hydrolysis of a native xylan containing galacturonic acid branches [31].

Space-filling molecular model of a sulfated oligoxylan sequence with one GlcA branch

The molecular structure(s) that underlies the multifunctional and heparin-like capacities of sulfated xylan remain undetermined, despite the importance that these agents have reached presently in the development of drugs against various human diseases. As noted above, the sulfated xylan is still too often looked upon generally as linear chains built up by β1,4 xylose to form a conformation like cellulose where each sugar ring is staggered 180 degrees by the β bonds, without any consideration of the α1,2 4OMe-D-GlcA linkages [e.g., 23, 40]. These considerations may be compared with those of the heparin chain. In contrast with 1,4-β linked oligoxylose, heparin is built up of sulfated disaccharide units consisting of an α1,4 D-glucosamine and a uronic acid (mainly α1,4 L-iduronic acid but some β D-GlcA). By virtue of the α D-linkage, the heparin chain tends to turn the disaccharides in a two-fold helical fashion [64, 65]. This turning can produce grooves as the sugars rotate 360 degrees about the axis. The carboxyl groups of the O_2 sulfated-α-L iduronic acid moieties would be disposed between the helically ordered sulfate groups that are located variably on the N_2, O_6, and possibly the O_3 positions of the glucosamines.

Bearing in mind that the xylan contains α 1,2 4OMe-D-GlcA branches and that some sulfated oligosaccharides in the Components may have multiple GlcA branches greater than the average number in the native xylan, we built a space-filling atomic model to examine the possible geometries of an α-linked D-GlcA relative to the 1,4-β linked pyranose chain and the neighboring sulfate groups on the xyloses. Figure 5 shows a photograph of a model sequence of seven xyloses containing an α1,2-linked 4OMe- D-GlcA branch on the central xylose. Sulfate groups on the C_2 and C_3 positions of the GlcA were omitted for clarity. The conformation of the 1,4-β xylose chain is illustrated by the view in the top panel. The bulky sulfate groups appear tightly packed into the space around the chain. The α D-GlcA (white bar) is out from the chain, turned towards the neighboring sugar. Turning the model ~ 90 degrees (middle

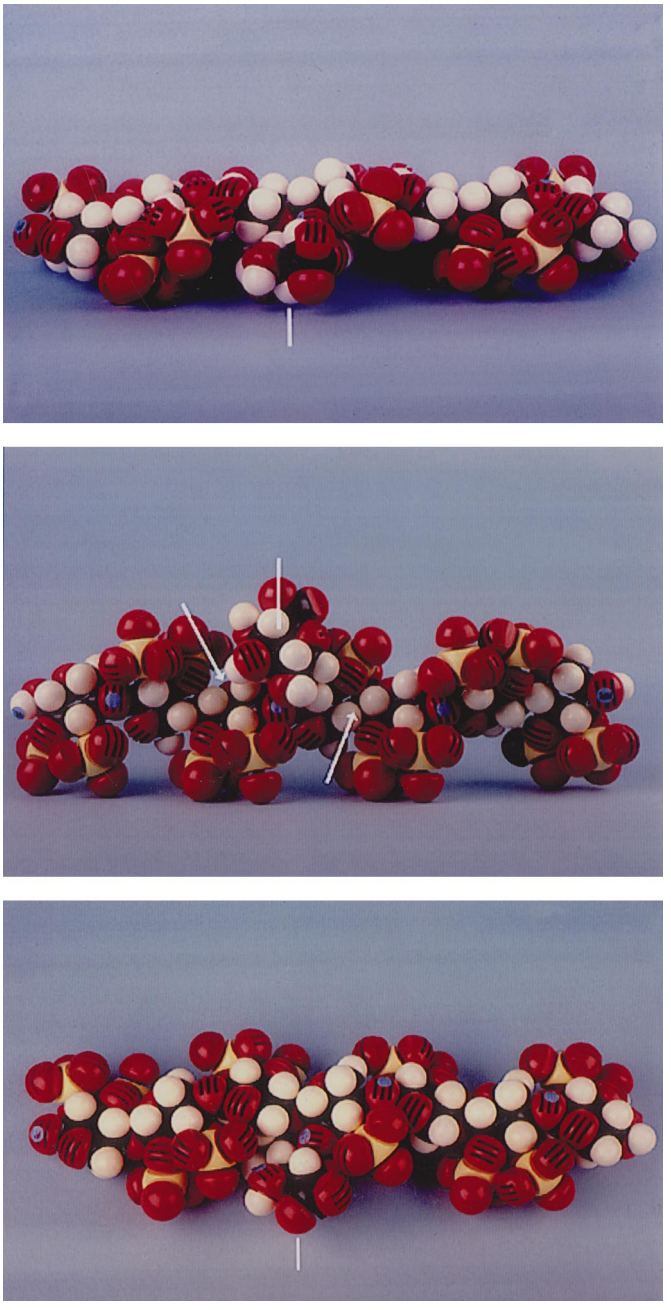

Figure 5. A space-filling atomic model of a sulfated xylan octasaccharide. The octasaccharide, reducing end (R) on the left, is a linear chain of seven sulfated xyloses in the pyranose form, and substituted on the O_2 position of the central xylose by a monomeric 4-OMe-GlcA branch. (The sulfates possible on O_2 and O_3 of the GlcA are omitted for clarity.) Xyloses are linked by 1–4 β bonds and the GlcA by a 1,2 α bond: sulfur, yellow; carbon, black; oxygen, red; hydrogen, white; blue circles mark the glycosidic bonds. *Top*: a view of the model that shows the β 1–4 glycosidic chain conformation of the linear hepta-xylose; white bar points to the GlcA branch. *Middle*: view of the model rotated by $\sim$90 degrees from that above; white bar points to GlcA; white arrows point to grooves. *Bottom*: a view looking down on the model in the middle panel.

panel) illustrates that the uronic acid carboxyl is positioned between sulfates located on both sides of the chain. The α-linkage twists the GlcA back towards the chain in a turn which, in concert with the sulfated xylose chain, creates several grooves (white arrows). The model illustrates the possibility that each GlcA may impart a localized turning to the anionic array of the sulfate groups nearby the carboxyl group. Looking down on the model (bottom panel), the relative geometries of the sulfates and carboxyl group are viewed from an aspect on the other side of the octasaccharide surface. The GlcA moiety need not contribute directly to enhance the binding strength of the oligoxylan in its antiviral or other pharmaceutical functions; it may supervene between other groups to stabilize a configuration that contributes to high affinity [9].

Our speculation that the capacity of sulfated xylan to mimic the specificities of heparins might be endowed by local conformational features involving its GlcA moieties and/or a particular array of its sulfate and carboxyl groups [41], despite the dissimilarities between their primary chain structures, is consistent with these considerations.

Discussion

Heparins and heparan sulfates have been notable as modulators of protein and cell membrane functions in numerous physiological processes. The structural specificity of functional domains in heparins was discovered by Rosenberg and coworkers with anticoagulantly active heparins [5]. These studies began to unravel the complex structural biology associated with the numerous functional specificities of this remarkable class of sulfated glycans. In particular, only a small portion of the heparin preparation binds tightly to antithrombin and is highly anticoagulantly active. Subsequent studies showed that this capacity is endowed by a unique antithrombin-binding hexasaccharide which resides within a specific 18 to 20-saccharide heparin sequence that is required for full heparin-activation of antithrombin against the clotting enzymes [4, 9]. Based on these findings and a tentative sequence derived from a spectroscopic study [30] of such a heparin octadecasaccharide, we have speculated that the heparins assume a basic structural formulation of helically-patterned disaccharide repeats (which occurs in solution [64] as well as in oriented fibers [65]). Many unique geometric arrays of sulfate and carboxyl groups confined to this molecular pattern could be predicted, and these subtle differences in structure would be sufficient to enable the numerous specificities in the functions of heparins.

After heparin was found to inhibit the *in vitro* infectivity of HIV-1 [18–20], several studies addressed the question of specificity among heparins and whether the anticoagulantly active and the highly HIV-1 inhibitory heparins could be differentially identified and separated physically or by

various chemical derivatizations [21, 22, 35, 67, 68]. Attempts to separate a highly active heparin with insignificant anticoagulant activity on the basis of physical and/or biochemical properties have been inconclusive. Although it is probable that this capacity would reside in a fraction having high affinity for a binding protein on the viral or target cell membrane, comprehensive studies have been lacking. The results of numerous modes of chemical derivatization of heparins, however, produced selective loss of anticoagulation capacity in several derivatives which displayed high anti-HIV-1 activity (EC_{50}s $= \sim 0.1$ to $7\,\mu g\,ml^{-1}$) [67], but there is currently no heparin agent in clinical use against AIDS.

AIDS is presently incurable. It may be arrested for various periods of time by nucleoside analogs and viral protease inhibitors and their combinations (which inhibit viral replication), but it has been inexorably fatal. The sulfated polysaccharide agents are thought to inhibit HIV mainly at the molecular mechanisms of viral binding to the target-cell [69], which would prevent virus entry into the cell. In the case of the antithrombotic sulfated xylan, the pharmaceutical is characterized by the supplier as having an average molecular weight of 4000–6000, much lower than $\sim 24{,}000$ which would be expected from sulfation of the native xylan ($= \sim 70$ xylose units). This signals that a high degree of heterogeneity was produced by an uncharacterized depolymerization during the sulfation process. Such heterogeneity and toxic effects have limited the level of clinical dosage of agents such as SP54 and probably have contributed to the puzzlingly poor or unimpressive correlations between the findings *in vitro* and clinical results in AIDS and cancers [37–40]. This has led to some bias against further inquiry into the potential of this class of antiviral agent. The limited clinical usefulness of sulfated xylans in AIDS has been attributed also to a failure of the agent to inhibit the virus in tissues where it is harbored [23]. Our hypothesis has been that the varied functional specificities of heparins might be mimicked by differing oligosaccharides in the heterogeneous mixture. A mechanism driven by specificity would provide rationale for overcoming the clinical limitations of such agents against AIDS and cancers, while a largely non-specific mechanism, based on the highly anionic nature of sulfated xylans, would not.

In the present study, we addressed the question of possible structural specificity in the inhibition of HIV-1 by heparin-like sulfated oligosaccharides. We used the sulfated xylan pharmaceutical as a model system because it is a readily available, inexpensive, chemically sulfated plant polysaccharide that has exhibited potent anti-HIV activity and a broad range of heparin-mimetic capacities. Numerous Components of this heterogeneous mixture were isolated chromatographically by permeation through BioGel P10 in 0.5 M ammonium bicarbonate. The separation of sulfated oligoxylans in this high salt eluant, which minimizes their interactions with the gel, would be mainly on the basis of mass, but the possible variations in sugar composition and anionic geometry and density among the oligosaccharides in this poorly defined mixture may also affect their relative separations. The Components were characterized by metachromatic absorption spectroscopy, ultracentrifugal analysis of dansyl derivatives using ultraviolet absorption optics, analysis of uronic acid content, and by comparative *in vitro* assays of potency against the cytotoxic and syncytium-forming infectivity of HIV-1.

The results of these initial studies reproducibly supported the idea that the inhibition of HIV-1 by sulfated xylan oligosaccharides requires a degree of molecular specificity. This is based on the dose-dependent, differential anti-HIV-1 potency displayed by the various Components against the cytotoxicity and syncytium-forming infectivity of HIV-1 *in vitro*: (1) High anti-cytotoxicity potency was associated with two structures, one was contained in Components eluting in the region of relative mass $\geqslant \sim 5500$ and the other was in a small oligomer about the size of a monomer; (2) High capacity for inhibition of syncytium-formation resided in oligosaccharide structure(s) which exhibited a minimum mass associated with the $\sim$ tetradecamer region. The significance of this apparent difference in minimum size required for inhibition of the two direct cell-killing effects by HIV-1 is unclear and further studies of oligosaccharides eluting in the mass range ~ 5500 to ~ 4000 would be needed to examine whether different structures were involved; (3) High anionic density was a characteristic of the relatively inactive Components as well as the highly active Components from nearby mass regions. A small Component characterized by a high anionic strength was also inactive.

These results suggest that certain oligosaccharides in the sulfated xylan preparation have structure(s) that may specifically act to inhibit the reactions between the virus envelope and the target cell membrane, that this action may also be heparin-mimetic in mechanism, and that non-specific inhibition due to high charge alone is unlikely to explain the anti-HIV-1 effects of the sulfated xylan mixture.

Membrane heparan sulfate and heparin have been implicated in the activation of basic fibroblast growth factor to a high affinity ligand for its cell receptor, where conceptually, heparan sulfate serves as a "low affinity receptor" and interacts with the growth factor in a specific manner; the structure of this functional sequence has been studied [13, 14, 70]. It is of interest here that Berger and coworkers now have shown that in addition to the CD4 cell receptor requirement for HIV-1 entry into the target cell, a second lymphocyte receptor, fusin, is also required for the fusion process [71]. Moreover, the fusin cofactor for the CD4-macrophage-tropic HIV-1 appears to be a receptor for a chemokine, CKR5 [72].

As noted above, the isolation of Components from the various chromatographic mass regions may encompass a superimposed distribution of oligosaccharides that contain different compositional and/or anionic geometries, and

these may be related to the observed differential potencies. The results of our analyses for GlcA content of the various chromatographic fractions and Components are the first to show that the ratio of GlcA to xylose is much higher than thought from the ratio of these constituents in the native xylan. Stabilization of the nearby glycosidic bond by the presence of a GlcA branch might have occurred in an otherwise random depolymerization of the xylan during the process of sulfation. The significance of the GlcA moietites in the anti-HIV-1 capacity of the Components is unknown, but these data raise the possibility that they might be structurally important. Further investigation of the GlcA constituents in the Components is necessary and in progress.

The physicochemical methods used in this study were readily adapted to highly sulfated oligosaccharides. A series of monodansylated-mass reference Components were produced and characterized as to weight average molecular mass by equilibrium ultracentrifugal analyses. These data indicated relatively narrow distributions of mass and the absence of dimer-or oligomerization in the samples: samples, in high salt (0.5 M NaCl) and at low concentration, displayed concentration distributions indistinguishable from that of homogeneous ideal solutes. Although dansyl derivatives of small oligosaccharides (< 2000) would tend to aggregate in the 0.5 M NaCl solvent (e.g., Component 16), this might be avoidable at lower salt concentrations. Analysis of the underivatized oligosaccharides directly was limited by their lack of major absorption above 200 nm. Analysis directly by scanning at 190 nm in the Beckmann XL-A ultracentrifuge might be applicable, but absorption of the light by the high salt solvent could pose major technical difficulties not present in the analysis used with the monodansylated derivatives. A study now ongoing using the XL-A indicated that analysis of such underivatized oligosaccharides would be possible using an absorption wavelength of 230 or 215 nm. In this analysis, the distributions of mass of the underivatized standards were, as with the dansyl derivatives, relatively narrow. Preliminary ^{1}H-NMR spectra of various Components indicated chemical shifts similar to the α- and β-anomeric and other hydrogens reported for unsulfated xylan oligosaccharides [73], but the expected splitting (coupling) was not displayed.

Recent studies on the origin and duration of HIV and HIV-infected CD4 lymphocytes in the plasma of AIDS patients have highlighted the magnitude of virus cleared from plasma each day: the plasma virus was derived from newly infected cells and was eliminated at about $0.05–2.0 \times 10^9$ virions per day with a half-life of ~ 2 days [74, 75]. Considering that the anti-HIV-1 capacity of sulfated xylan was governed by a degree of structural specificity, separation of highly active antiviral oligosaccharides from those having unwanted heparin-mimetic functions such as anticoagulant capacity might be feasible [76]. A relatively specific anti-HIV-1 sulfated oligosaccharide might produce a protective interceptor effect against infectivity of HIV-1 clinically because of an increase in tolerance of high and repeated doses, particular routes of administration, select targets for protection against vertical transmission, and/or combination with present combination regimes that have different modes of viral inhibition.

In this first study, we began an examination of the structure-function relation of the heparin-mimetic sulfated xylan, especially as it might relate to its inhibition of the *in vitro* cytotoxic and syncytium-forming infectivity of HIV-1. A major question was whether the inhibition was nonspecific or whether there was a structural specificity required in the molecular interactions. We found that there was a degree of structural specificity underlying this capacity of sulfated xylan. In addition, a structural feature of the sulfated xylan oligosaccharides, an unexpectedly high GlcA content, was noted. These findings would have general significance in the drug development strategies applied to the increasing biomedical potentials of sulfated xylans. Elucidation and extension of the initial findings on the structure-function relations of the sulfated xylan oligosaccharides would require development of an upscaled preparation, additional purification of the anti-HIV-1 Components and study of their structural properties by applying additional spectroscopic techniques, and medium and high pressure chromatography, which we are currently pursuing.

Acknowledgment

The authors are grateful to Dr. Dominique Schols (bene-Arzneimittel, Munich) for the supply of SP54, and are pleased to acknowledge the contribution of Dr. Ven Narayanan, Ms. Nancy Dunlop, and Drs. Owen Weislow and Robert Shoemaker (National Cancer Institute) in their cooperation and discussions in conducting the anti-viral bioassays. We thank Dr. John Robbins for his encouragement and suggestions.

References

1 Silbert JE (1967) *J Biol Chem* **242**: 5146–52.
2 Lindahl U, Hook M, Backstrom G, Jacobsson I, Reisenfeld J, Malstrom A, Roden L, Feingold DS (1977) *Fed Proceedings* **36**: 19–24.
3 Leder IG (1980) *Biochem Biophys Res Commun* (1980) **94**: 1183–9.
4 Bourin M-C, Lindahl U (1993) *Biochem J* **289**: 313–30.
5 Lam LH, Silbert JE, Rosenberg RD (1976) *Biochem Biophys Res Commun* **69**: 570–7.
6 Rosenberg RD (1977) *Fed Proceedings* **36**: 10–17.
7 Rosenberg RD, Jordan RE, Favreau LV, Lam LH (1979) *Biochem Biophys Res Commun* **86**: 1319–24.
8 Oosta GA, Gardner WT, Beeler D, Rosenberg RD (1981) *Proc Natl Acad Sci USA* **78**: 829–33.
9 Rosenberg RD, Bauer KA, Marcum JA (1986) *Rev of Hematology* **2**: 351–416.
10 Savion N, Vlodavsky I, Fuks Z (1984) *J Cell Physiol* **118**: 169–78.

11 Herbert JM (1991) *Biochim Biophys Acta* **1091**: 432–41.
12 Yayon A, Klagsbrun M, Esco J, Leder P, Ornitz DM (1991) *Cell* **64**: 841–8.
3 Walker A, Turnbull JE, Gallagher JT (1994) *J Biol Chem* **269**: 931–5.
14 Sasaki S, Suchi T (1967) *Nature* **216**: 1013–14.
15 Brenan M, Parish CR (1986) *Eur J Immunol* **16**: 423–30.
16 Bradbury MG, Parish CR (1991) *Immunol* **72**: 231–8.
17 Caughey B, Brown K, Raymond GJ, Katzenstein GE, Thresher W (1994) *J Virol* **68**: 2135–41.
18 Bagasra O, Lischner HW (1988) *J Infec Dis* **158**: 1084–7.
19 Baba M, Nakajima M, Schols D, Pauwels R, Balzarini J, De Clercq E (1988) *Antiviral Res* **9**: 335–43.
20 Ueno R, Kuno S (1987) *Lancet* **1**: 1379.
21 Baba M, Pauwels R, Balzarini J, Arnot J, Desmyter J, De Clercq E (1988) *Proc Natl Acad Sci USA* **85**: 6132–6.
22 Coombe DR, Harrop HA, Watton J, Mulloy B, Barrowcliffe TW, Rider CC (1995) *AIDS Res and Hum Retroviruses* **11**: 1393–6.
23 Witvreuw M, Desmyter J, De Clercq E (1994) *Antiviral Chem & Chemother* **5**: 345–59 (Review).
24 Lederman S, Gulick R, Chess L (1989) *J. Immunol* **143**: 1149–54.
25 McClure MO, Moore JP, Blanc DF, Scotting P, Cook JMW, Keynes RJ, Weber JN, Davies D, Weiss RA (1992) *Aids Res & Hum Retroviruses* **8**: 19–26.
26 Baba M, Schols D, Pauwels R, Nakashima H, De Clercq E (1990) *J Acquired Immune Defi Dis* **3**: 493–9.
27 Zugmaier G, Lippman ME, Wellstein A (1992) *J Natl Cancer Inst* **84**: 1716–24.
28 Meri S, Pangburn MK (1994) *Biochem Biophys Res Comm* **198**: 52–9.
29 Koistinen V (1993) *Mol Immunol* **30**: 113–18.
30 Stone AL (1985) *Arch Biochem Biophys* **236**: 342–53.
31 Stscherbina D, Philipp B (1991) *Acta Polym* **42**: 345–51 (Review).
32 Pienta KJ, Murphy BC, Issacs JT, Coffey DS (1992) *Prostate* **20**: 233–41.
33 Caughey B, Raymond GJ (1993) *J Virol* **67**: 643–50.
34 Ladogana A, Casaccia P, Ingrosso L, Cibati M, Salvatore M, Xi YG, Masullo C, Pocchiari M (1992) *J Gen Virol* **73**: 661–5.
35 Baba M, De Clercq E, Schols D, Pauwels R, Snoeck R, Van Boeckel C, Vandedom G, Kraaileveld N, Hobbelen P, Ottenheim H, Den Hollander F (1990) *J Infec Dis* **161**: 208–13.
36 Abrams I, Kuno S, Wong R, Jeffords K, Nash M, Molaghan JB, Gortner R, Ueno R (1989) *Ann Inter Med* **10**: 183–8.
37 Pluda JM, Shay LE, Foli A, Tannenbaum S, Cohen PJ, Goldspeil BR, Adamo D, Cooper MR, Broder S, Yarchoan R (1993) *J Natl Cancer Inst* **85**: 1585–92.
38 Swain SM, Parker B, Wellstein A, Lippman ME, Steakley C, DeLap R (1995) *Invest New Drugs* **13**: 55–62.
39 Marshall JL, Hawkins MJ (1995) *Breast Cancer Res & Treatment* **36**: 253–61.
40 Stone AL, Melton DJ (1991) *Glycoconjugate J* **8**: 175.
41 Stone AL, Spitzin SV, Melton DJ (1992) *Glycobiology* **2**: 468.
42 Raveux R, Gros P, Briot M (1965) *Bull Soc Chim Fr* **33**: 2744–9.
43 Aspinall GO, Hirst EL, Mahomed J (1954) *J Chem Soc* 1734–41.
44 Constantopoulos G, Dekaban AS, Carroll WR (1969) *Anal Biochem* **31**: 59–70.
45 Stone AL, Childers LG, Bradley DF (1963) *Biopolymers* **1**: 111–31.
46 Stone AL, Bradley DF (1967) *Biochim Biophys Acta* **148**: 172–92.
47 Stone AL, Szu SC (1988) *J Clin Microbiol* **26**: 719–25.
48 Stone AL (1981) In *Chemistry and Biology of Heparin* (Lunbad RL, Brown WV, Mann KG, Roberts HR, eds) pp 143–56, New York: Elsevier/North Holland.
49 Weislow OS, Kiser R, Fine DL, Bader J, Shoemaker RH, Boyd MR (1989) *J Natl Cancer Inst* **81**: 577–86.
50 Nara PL (1990) In *Techniques in HIV Research*, Aldovini A, Walker B, eds, pp 77–86, New York: Stockholm Press.
51 Avigad G (1977) *J Chromatog* **139**: 343–7.
52 Lewis MS (1992) In *Analytical Ultracentrifugation in Biochemistry and Polymer Science*, Harding SE, Rowe AJ, Horton JC, eds, pp 126–37, London: Royal Society of Chemistry.
53 Zamyatnin AA (1984) *An Rev Biophys Bioeng* **13**: 145–65.
54 Durchshlag H (1986) In *Thermodynamic Data for Biochemistry and Biotechnology*, Hinz H-J, ed, pp. 45–128, New York: Springer-Verlag.
55 Lasker, SE (1965) *Some properties of fractionated heparin*: Dissertation, ed. University Microfilms, Inc. (Ann Arbor, MI).
56 Jordan RE, Favreau LV, Braswell EH, Rosenberg RD (1982) *J Biol Chem* **257**: 400–6.
57 Knott GD (1979) *Comput Programs Biomed* **10**: 271–80.
58 Williams JW, Van Holde KF, Baldwin RL, Fujita H (1958) *Chem Rev* **58**: 715–806.
59 Hoare DG, Koshland DE (1967) *J Biol Chem* **242**: 2447–53.
60 Horikawa R, Tanimura T (1982) *Anal Lett* **15**: 1629–42.
61 Bystricky S, Szu SC (1994) *Biophys Chemistry* **50**: 1–7.
62 Stone AL (1967) *Biochim Biophys Acta* **148**: 193–206.
63 Stone AL, Spitzin SV, Melton DJ (1993) *Glycobiology* **3**: 520.
64 Stone AL (1964) *Biopolymers* **2**: 315–325.
65 Atkins TE (1977) *Fed Proceedings* **36**: 78–83.
66 Bitter T, Muir HM (1962) *Anal Biochem* **4**: 330–4.
67 Barzue T, Level M, Petitou M, Lormeau J-C, Choay J, Schols D, Baba M, Pauwels R, Witvrouw M, De Clerq E (1993) *J Med Chem* **36**: 3546–55.
68 Lopalco L, Ciccomascolo F, Lanza P, Zoppetti G, Caramazza I, Leoni F, Beretta A, Siccardi AG (1994) *AIDS Res & Hu Retroviruses* **10**: 787–93.
69 Nara P, Garrity RR, Goudsmit J (1991) *FASEB J* **5**: 2437–55.
70 Faham S, Hileman RE, Fromm JR, Linhardt RJ, Rees DC (1996) *Science* **271**: 1116–20.
71 Feng Y, Broder C, Kennedy PE, Berger EA (1996) *Science* **272**: 872–7.
72 Alkhatlb G, Combadiere C, Broder C, Feng Y, Kennedy PE, Murphy PM, Berger EA (1996) *Science* **272**: 1955–8.
73 Hoffmann RA, Leeflang BR, deBarse MMJ, Amerling JP, Vliegenthart (1991) *Carbohydr Res* **221**: 63–81.
74 Wel S, Ghosh S, Taylor ME, Johnson VA, Emini EA, Deutsch P, Lifson JD, Bonhoeffer S, Nowak MA, Hahn BH, Saag MS, Shaw GM (1995) *Nature* **373**: 117–22.
75 Ho DD, Neuman AU, Perelson AS, Chen W, Leonard JM, Markowitz M (1995) *Nature* **373**: 123–6.
76 Stone AL, Melton DJ, Horne MK (1996) *Glycobiology* **6**: 773.

Received 25 June 1997, revised 29 September 1997, accepted 20 October 1997